Article

Comparison of Culture Media for *in-vitro* Expansion of Oral Epithelial Keratinocytes: Implications for Testing E-liquid Flavors

Giancarlo Cuadra[1*], Abrar Shamim[1,2], Raivat Shah[1], Joey Morgan[3], and Dominic Palazzolo[4]

[1] Department of Biology, Muhlenberg College, 2400 W. Chew Street, Allentown, PA, 18104, USA;
[2] Columbia University College of Dental Medicine, New York, NY, USA;
[3] College of Veterinary Medicine, Lincoln Memorial University, Harrogate, TN 37752, USA;
[4] Department of Physiology, DeBusk College of Osteopathic Medicine, Lincoln Memorial University, Harrogate, TN 37752, USA.
* Correspondence: giancarlocuadra@muhlenberg.edu (484) 664 3256

Abstract: Background: Understanding *in vitro* expansion of OKF6/TERT-2 oral epithelial cells is important for studying molecular biology of disease and pathology affecting the oral cavity. The media used for any cell culture is paramount in terms of efficient output. Therefore, this study aims to compare two different media for OKF6/TERT-2 cultures: Keratinocyte Serum-Free Medium (KSFM) and a composite medium comprised of DMEM/F-12 mixed with KSFM (referred to as DFK). For application purposes, this investigation also compares the toxicological effects of flavored electronic cigarette liquids (E-liquids) on OKF6/TERT-2 cultures grown in both media. **Methods**: Cells were grown in KSFM and DFK media and cellular growth, morphology, gene expression of mucins and tight junctions, as well as wound-healing were determined. Additionally, cellular viability and cytotoxicity were indexed after E-liquid exposures. **Results**: While overall cellular morphologies remained unaltered, cells grown in DFK reached confluency faster. Except for *claudin-1*, there is no appreciable difference in expression of the other genes tested. Additionally, cultures in DFK appear more sensitive to E-liquids ± flavors. **Conclusions**: DFK is an alternative medium for cultivation of OKF6/TERT-2 cells to study molecular biology of disease and pathology, such as their responses to E-liquids ± flavors.

Keywords: oral; mucosa; mucins; tight junctions; wound-healing; E-liquids; cytotoxicity; viability; confluency

1. Introduction

The epithelial lining of the oral mucosa is a critical barrier protecting the subepithelial and distal airway tissues from the environment and is one of the first mucosal surfaces that ingested substances encounter. The early exposure of cells in the upper respiratory tract and oral cavity makes them a valuable tool for studying biology, to include, but not limited to pathophysiology, host-microbe interactions, innate immunity, toxicology, and pathology. OKF6/TERT-2 cells are oral mucosal epithelial keratinocytes, isolated from a human male, that have been immortalized via telomerase 2 retroviral transduction and expression, as well as deletion of the p16INK4a regulatory protein [1]. The OKF6/TERT-2 cell line has shown significant research utility, with publications using these cells to investigate topics including but not limited to carcinogenesis of oropharyngeal malignancy [2–4], infectious disease [5], periodontal disease [6,7], and various tobacco products such as conventional cigarettes [8], shisha [9], and chewable tobacco [10].

Keratinocyte serum-free medium (KSFM) is a culture medium optimized for the growth of human keratinocytes that is widely used to culture epithelial cell lines ranging from hepatocytes [11], to urothelial cells [12], to corneal epithelial cells [13]. This me-

Preprints (www.preprints.org) | NOT PEER-REVIEWED | Posted: 9 January 2023 doi:10.20944/preprints202301.0150.v1

dium, commonly containing 0.09 mM calcium supplemented with 30 μg/ml pituitary bovine extract, 0.2 ng/ml EGF, 10% FBS, and ampicillin/streptomycin, has been the primary medium for culturing OKF6/TERT-2 cells in current literature. [5,7,14–16]. Dickson et al. [1] described a protocol in which this cell line was cultured in KSFM, which has since been widely cited and replicated [17–21]. Dulbecco's Modified Eagle Medium/Nutrient Mixture of Hams F-12 (DMEM/F-12) is another standard basal medium commonly containing 1.05 mM calcium [22]. DMEM/F-12, supplemented with 10% fetal bovine serum (FBS), 100 U/mL penicillin, and 100 μg/mL streptomycin is used for the culture of a wider spectrum of cells, including fibroblasts, neurons, muscle cells, and cell lines including HeLa [22]. DMEM/F-12 with 10% FBS has less frequently been used to culture OKF6/TERT-2 cells [23,24]. Most other studies have used the KSFM methodology as described by Dickson et al. [1]

OKF6/TERT-2 cells were originally established in KSFM with its own set of nutrients, but DMEM/F12, which consists of a different set of nutrients, has also been used. Cell access to both sets of nutrients may increase their growth conditions. The justification for a comparison of the growth of the OKF6/TERT-2 cell line in KSFM and a 1:1 v/v mixture of DMEM/F-12 and KSFM, from this point on referred to as DFK, is two-fold: First, to establish that these two media support the growth of OKF6/TERT-2. Second, to determine potential benefits, such as associated costs and the time to reach confluency, which would ultimately impact the use of this cell line. We note that other orally-derived cell lines, such as human gingival fibroblasts [25,26], dental pulp stem cells [27], and normal human epidermal keratinocytes [28] are more commonly cultured on DMEM/F-12. As such, the combination medium (i.e., DFK) for the growth of OKF-6/TERT-2 oral epithelial cells may provide other groups with increased flexibility for cell culturing.

In addition to comparing growth characteristics, including time-to-confluency and morphology of OKF6/TERT-2 cells in KSFM and DFK, the functional characteristics of these cells should also be measured to evaluate a viable alternative culture medium. Similar to epithelial cells from other anatomic sites, the barrier function of the oral epithelium is critical in maintaining a well-defined "inside" vs. "outside" environment by demarcating the apical and basolateral domains of adjacent cells in the superficial mucosa[29]. This is accomplished through functional protein complexes known as tight junctions, which include claudin-1, occludin, and zonula occluden protein 1 (ZO-1). These tight junctions assist in an array of functions, including the regulation of paracellular transport, cell polarity, and importantly, sustaining the functional semipermeable barrier of the oral epithelium [30]. Another barrier function is the ability to close wounds after mechanical injury, which helps prevent microbial and environmental hazards from reaching the connective tissue.

Within the oral cavity, after swallowing, roughly 800 μL of saliva remain on oral surfaces [31], providing lubrication and moisture. Of this, 5 to 10% of the dry weight is composed of mucin glycoproteins, a major component of the saliva [32,33], as well as the respiratory [34] and GI tracts [35]. At least 20 mucins have been identified in the saliva that are functional protective substances that play a role in salivary flow and composition and therefore dysregulation may increase susceptibility to pathogens, such as *Candida albicans* [36], and dental decay [37]. Mucin glycoproteins are expressed by a wide range of epithelial cells, typically on the apical membrane and as a gelatinous component or as a lubricant and protective agent in the saliva [38,39]. Mucins play a pivotal role in cellular growth, differentiation, and signaling, as well as homeostasis and innate immunity within the oral cavity [38,39]. Mucin genes such as *muc1* and *muc4* are expressed broadly in epithelial cells of the body, including the upper aero-respiratory tract and oral cavity [40]. Over- and under-expression of mucin genes and other modifications, such as aberrant glycosylation, have been implicated in situations of epithelial dysfunction, including malignant transformation [41,42] and breakdown of the nasal epithelial barrier [43]. For the OKF6/TERT-2 cell model to be representative of *in vivo* physiology, the production of mucins should

Preprints (www.preprints.org) | NOT PEER-REVIEWED | Posted: 9 January 2023 doi:10.20944/preprints202301.0150.v1

remain consistent. Therefore, comparable expression of the *muc1* and *muc4* genes, in conjunction with tight junctions, will be used to further assess the functional equivalency of the OKF6/TERT-2 cell line grown in KSFM and DFK media.

The OKF6/TERT-2 cell line has conventionally been cultured using a standard KSFM medium. However, the flexibility of this cell line to be cultured in other media, such as DFK, remains to be determined. The ability to diversify the growth and culture requirements of the OKF6/TERT-2 cell line amplifies its research potential. Therefore, the aim of this study is to compare KSFM and DFK as media that can support OKF6/TERT-2 cell cultures, analyzing growth, morphology, tight junctions, and mucin glycoproteins gene expression, as well as tissue repair. Exploring the effects of electronic cigarette liquids (E-liquids) ± flavors, which have previously demonstrated a significant impact on the oral microenvironment [44–51], is an important research direction. From a practical point of view, toxicological experiments were also performed using E-liquids ± flavors to determine which of these two media renders the cell cultures more suitable for such studies.

2. Results

2.1. Seeding OKF6/TERT-2 cells in KSFM or DFK

After attempting to seed OKF6/TERT-2 cells in KSFM or DFK, cells adhered well to the surface when seeded with the KSFM media, as seen by day 1 in Figure 1. Cells in KSFM present the correct morphology with pseudopodia extensions, forming small microcolonies in the well. By day 1, few cells remained adhered to the surface when seeded with DFK, and these cells appear rounded, with a different phenotype when compared to cells in KSFM. By day 2, however, cells cultured in DFK seem to present the correct morphology, with scarce microcolonies. On the other hand, by day 2, cells in KSFM are beginning to grow confluent, with a much higher cell number per field of view (Fig 1). Our results indicate that when seeding OKF6/TERT-2 cells, KSFM should be the medium used as it yields the correct phenotype and enhanced growth within one day, compared to DFK.

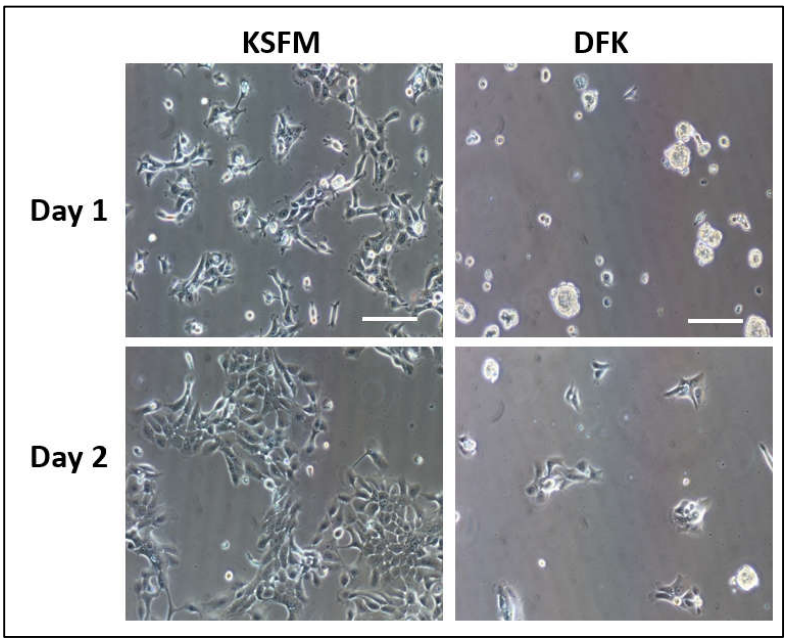

Figure 1. Light microscopy displaying cellular morphology and confluency of OKF6/TERT-2 cells seeded in KSFM and DFK media. Bar = 100 µm.

2.2. OKF6/TERT-2 seeded in KSFM and switched to DFK

OKF6/TERT-2 cells were seeded in KSFM and 24 hours later, they were either kept on this medium or switched to DFK for the remainder of the experiment. Throughout the entire experiment, the cell morphology appears to be similar regardless of the media used

Preprints (www.preprints.org) | NOT PEER-REVIEWED | Posted: 9 January 2023 doi:10.20944/preprints202301.0150.v1

(Fig 2A). However, the cellular confluency progresses slightly faster in the DFK cultures. Viable cell counts, performed by trypsinization and trypan blue exclusion, demonstrate a significant difference in viable cell numbers between the DFK and KSFM cultures as of day 2 (Fig 2B, $p < 0.001$) supporting the visual observation in Figure 2A. These results indicate that, although cultures in KSFM do reach confluency, a protocol of seeding with KSFM (day 0) and switching to DFK by day 1 is the most effective in terms of growth rate. For the remainder of the study, OKF6/TERT-2 cells seeded and maintained in KSFM are compared to cells seeded in KSFM and switched to DFK. The latter culture method is simply referred to as "DFK". Interestingly, by day 3 both cell cultures appear 100% confluent, but the cell number is nearly double in DFK cultures. These results may indicate that by day 3, cells in DFK could have switched to a cuboidal morphology or decreased in cellular size.

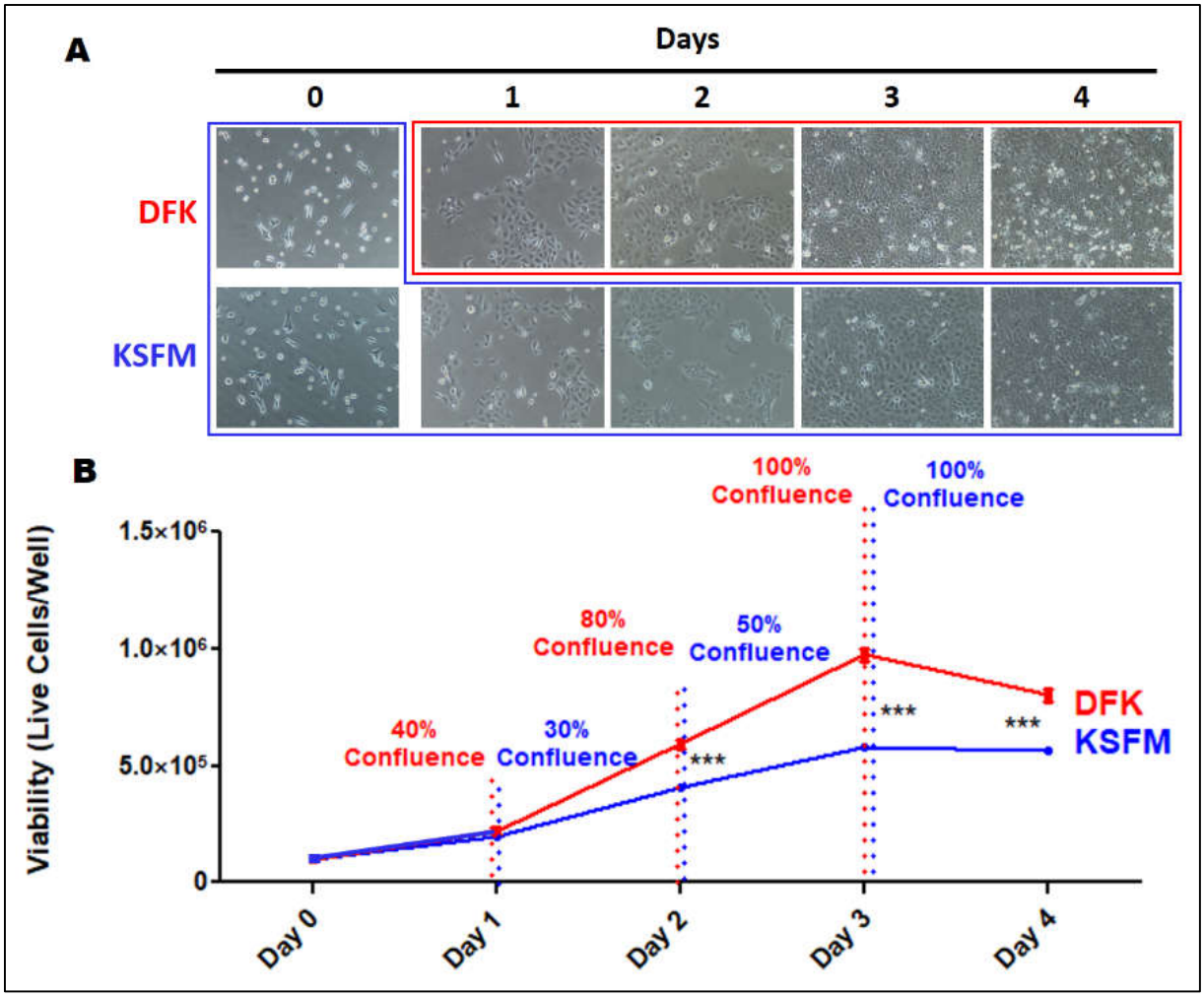

Figure 2. Light microscopy displaying cellular morphology and confluency of OKF6/TERT-2 cells seeded in KSFM and either kept in this medium or switched to DFK 24 hours later until the end of the experiment (A). Quantification of viable OKF6/TERT-2 cells in both media was measured via trypan blue exclusion (B). *** = $p < 0.001$.

2.3. Confocal analysis of OKF6/TERT-2 morphology after growth in DFK and KSFM

Mucosal epithelial cells are mainly of squamous morphology: high width to height ratio [52]. The results in Figure 2 could be explained by a change in DFK-cultured OKF6/TERT-2 cellular morphology, where the cells may elongate in height (i.e., cuboidal) or decrease their overall cellular size. If the cells adopt a more cuboidal phenotype, they will increase in height. Conversely, if the cells remain in a squamous morphology, they simply decrease in overall cellular size. To discern between these two possible outcomes,

Preprints (www.preprints.org) | NOT PEER-REVIEWED | Posted: 9 January 2023 doi:10.20944/preprints202301.0150.v1

confluent monolayers were stained with fluorescence and observed under confocal microscopy, yielding a quantification of the z-axis (height). OKF6/TERT-2 cells grown for four days in KSFM and DFK are shown in Figure 3A, where the left side shows two-dimensional images, and the right side shows three-dimensional views of the cultures. No conspicuous difference in morphology is observed. However, as shown in Figure 3B the number of cells per field of view is 1.73 times higher in DFK as compared to KSFM ($p < 0.001$), which agrees with the results in Figure 2. Figure 3C shows that the mean area of OKF6/TERT-2 cells in KSFM is significantly larger than cells in DFK ($p < 0.001$). The height, as indexed by Z-stacks (Fig 3D), reveals that cells reach roughly 13 μm in height with no significant difference observed between media. Furthermore, figure 3E show that cells grown in KSFM have a significantly higher cellular volume ($p < 0.001$). Consequently, our results favor the idea of a decrease in cell size. Overall, the results indicate the morphology of the cells remains squamous and does not change based on the media but the cells in DFK are smaller in size than those in KSFM. A potential explanation is that cells grown in DFK undergo mitosis faster and do not have enough time to accumulate cellular content, hence they are smaller and more numerous per surface area.

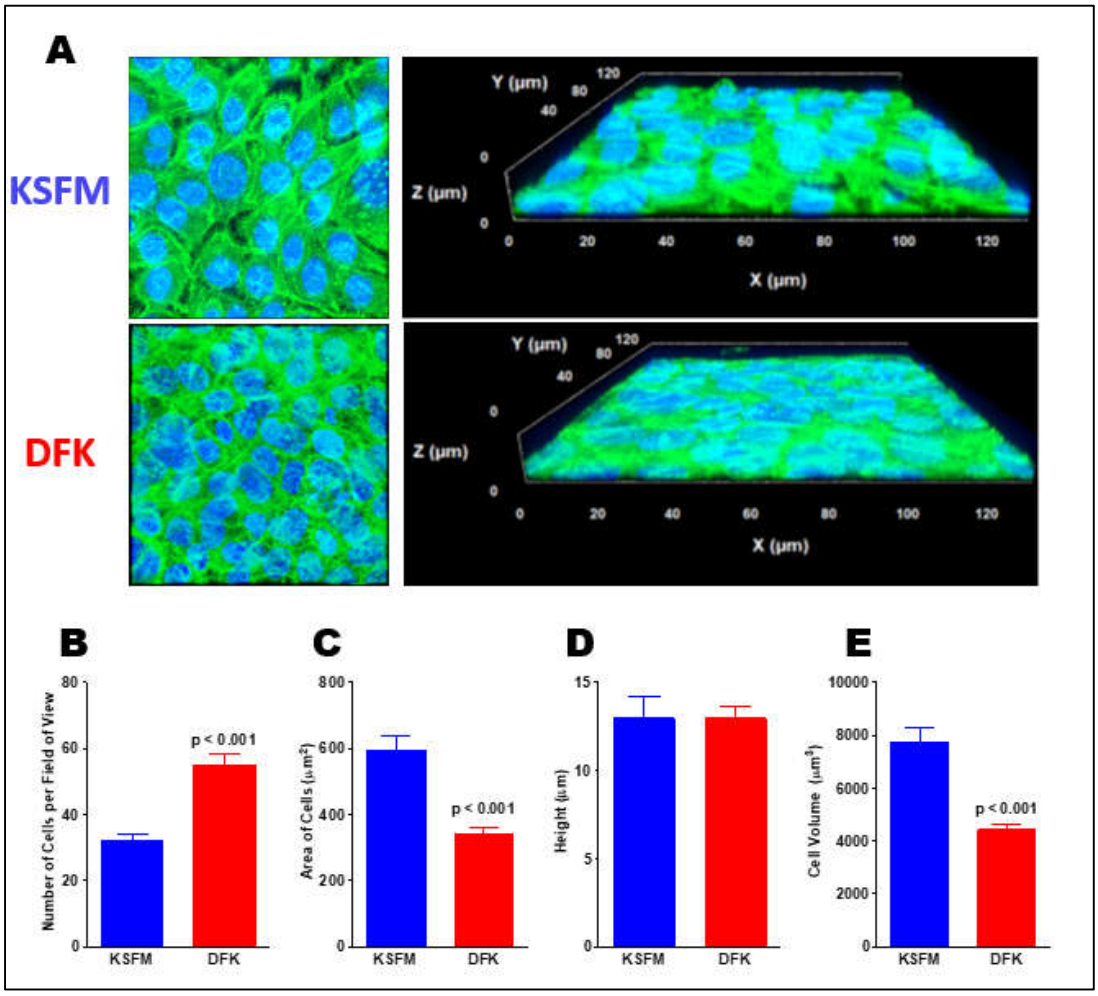

Figure 3. Confocal imaging and cellular size of confluent OKF6/TERT-2 cells grown in KSFM and DFK. Representative confocal (2D) images of cell cultures grown in KSFM and DFK by day 4. Phalloidin green labels actin filaments and DAPI blue labels cellular nuclei. Each frame is 135 μm per side, total magnification = 630X. Z-stacks were tilted to render 3D images (A). Mean number of cells per field of view ± SE in both media (B). Average area of cells ± SE (n = 8) was calculated by dividing the total area of the field of view by the mean number of cells (C). Average height ± SE (n = 17 to 18) of cells after growth in each media was indexed by the Z-stacks (D). Average cell volume ± SE was calculated by multiplying area (n = 8) times the average height of cells (E).

Preprints (www.preprints.org) | NOT PEER-REVIEWED | Posted: 9 January 2023 doi:10.20944/preprints202301.0150.v1

2.4. Expression of Mucins and Tight Junction genes after growth in DFK and KSFM

Oral epithelial cells have several functions, including the production of mucins and tight junctions. Both of these cellular factors aim to prevent foreign materials, such as microbial products or environmental hazards, from interacting directly with oral tissues. In the case of mucins, *muc1* and *muc4* are among the most abundant in oral epithelial tissues. Tight junction genes *occludin*, *claudin-1* and *ZO-1* yield the most important proteins of these structures. These genes were tested via qPCR and the results, presented in figure 4, are compared to the levels of β-actin expression in terms of percentages. OKF6/TERT-2 cells grown in DFK express a slightly higher level of *muc1* (3%) compared to their KSFM counterparts (1.8%), but this was not significant ($p < 0.08$). A much lower, but detectable level of *muc4* was found in these cells (0.01% in both cultures), once again, with no significant difference among them. For the tight junction genes, *ZO-1* was highly expressed in both cell cultures, with amounts of roughly 22 and 25% in KSFM and DFK, respectively (compared to β-actin). Interestingly, *claudin-1* was upregulated in cells grown in DKF to 28%, which is significantly different than the 4% found in KSFM ($p < 0.05$). Cells grown in both DFK and KSFM expressed about 4% of *occludin* with no significant difference among the different cultures. Taken together, OKF6/TERT-2 cells grown in DFK or KSFM express similar levels of *muc1*, *muc4*, *occludin* and *ZO-1*. However, the growth of OKF6/TERT-2 in DFK yields seven times higher expression of *claudin-1* compared to that in KSFM, suggesting a more robust formation of tight junctions in the former medium.

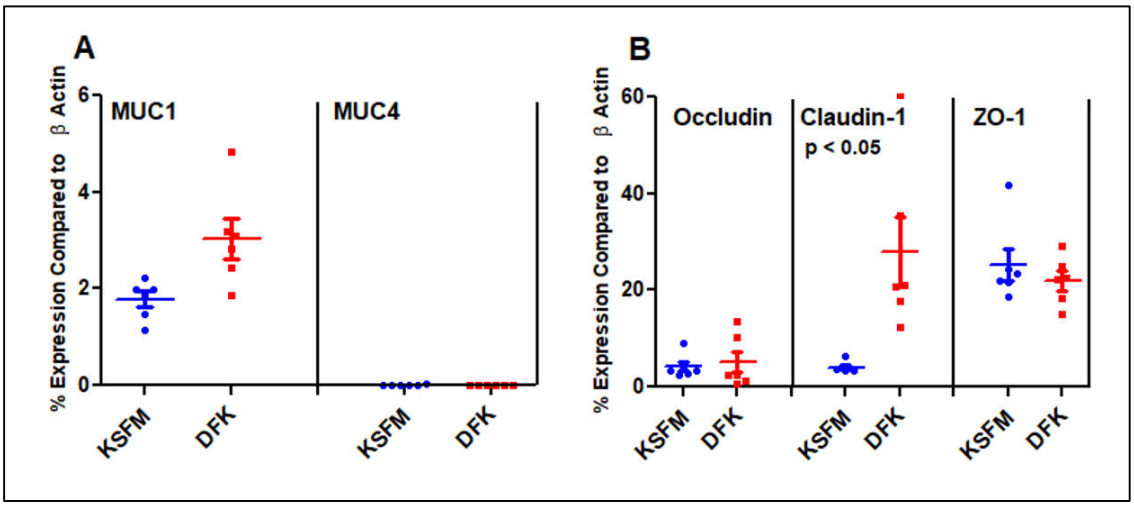

Figure 4. QPCR: Expression levels of mucins and tight junction genes compared to β-actin as a percentage. Horizontal lines represent the mean ± SE of six data points.

2.5. Release of Mucins after growth in DFK and KSFM

After quantifying roughly 1 to 4% expression of *muc1* compared to β-actin, the possibility that OKF6/TERT-2 cells could be releasing *muc1* glycoproteins into solution, as is the case with *in vivo* oral epithelial cells, was tested using SDS-PAGE. Because of the high levels of glycosylation, MUC1 travels very little in SDS-PAGE and would appear as a high molecular-weight (MW) band. To test whether mucins are released by OKF6/TERT-2 cells *in vitro*, supernatants from DFK and KSFM cultures were concentrated, separated by sodium dodecyl sulfite polyacrylamide gel electrophoresis (SDS-PAGE) and all glycoproteins were stained using the periodic-acid-Schiff (PAS) protocol, followed by Coomassie staining. Figure 5A shows high MW bands in the supernatants of both DFK and KSFM cultures (lanes 2 – 5), which correspond to the same high MW materials in human saliva (lanes 8 – 9). In addition, these bands are not observed in concentrates of fresh DFK or KSFM media (lanes 6 and 7), indicating that such high MW glycoproteins were produced and secreted by OKF6/TERT-2 cells during culture. Our results indicate that our cell

Preprints (www.preprints.org) | NOT PEER-REVIEWED | Posted: 9 January 2023 doi:10.20944/preprints202301.0150.v1

model, whether cultured in KSFM or DFK, mimics the behavior of *in vivo* oral epithelial tissues in terms of mucin production and secretion.

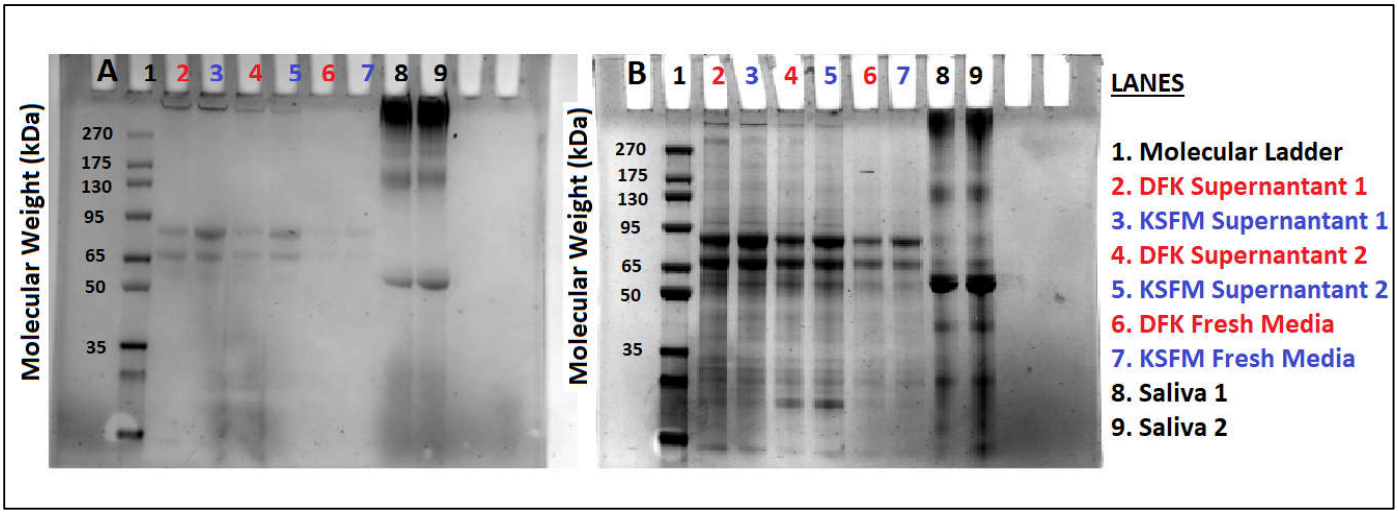

Figure 5. Concentrated materials from OKF6/TERT-2 cell culture supernatants in both KSFM and DFK (lanes 2 – 5), uncultured KSFM or DFK media (lanes 6 and 7) or human saliva (lanes 8 and 9) were separated by SDS-PAGE. PAS staining, specific for glycoproteins, reveals high molecular weight materials in saliva lanes and supernatants (A). Coomassie stain shows all proteins found in the same gel (B). Lanes 2 – 5 represent two independent experiments comparing KSFM vs. DFK culture supernatants. Each lane was loaded with 30 μg of protein.

2.6. Wound healing assay in DFK and KSFM

Another important function of oral epithelial cells is their ability to close wounds after injury, which also helps limit microbes, microbial products, or environmental materials from entering connective tissues or the bloodstream. A wound-heal assay comparing OFK6/TERT-2 cell culture open-wound recovery can provide insight into cell culture media preference regarding post-injury recovery rate and time until full confluence is achieved. OKF6/TERT-2 epithelial cells demonstrate a significantly greater wound recovery rate in DFK compared to cultures in KSFM (Figure 6A). After 25 h, cultures in DFK exhibited full closure while the KSFM counterparts still present small gaps (Figure 6A). Quantification of the gap size indicates a significant difference at 7, 12 and 20 hours of wound healing, where cells in DFK close the gap faster ($p < 0.05$). In addition, by 0 hours, there is a significantly greater gap in the DFK cultures ($p < 0.05$). Irrespective of this uneven start, cultures in DFK were able to heal much quicker and regression analyses indicate that (1) DFK and KSFM cultures completely recover by 23.4 hours and 39.2 hours, respectively, and (2) correlation coefficient R^2 values indicate that KSFM cultures may have a more of a non-linear recovery compared to DFK. Hence, under our conditions, the data suggest that OKF6/TERT-2 cells recover faster in DFK.

Preprints (www.preprints.org) | NOT PEER-REVIEWED | Posted: 9 January 2023 doi:10.20944/preprints202301.0150.v1

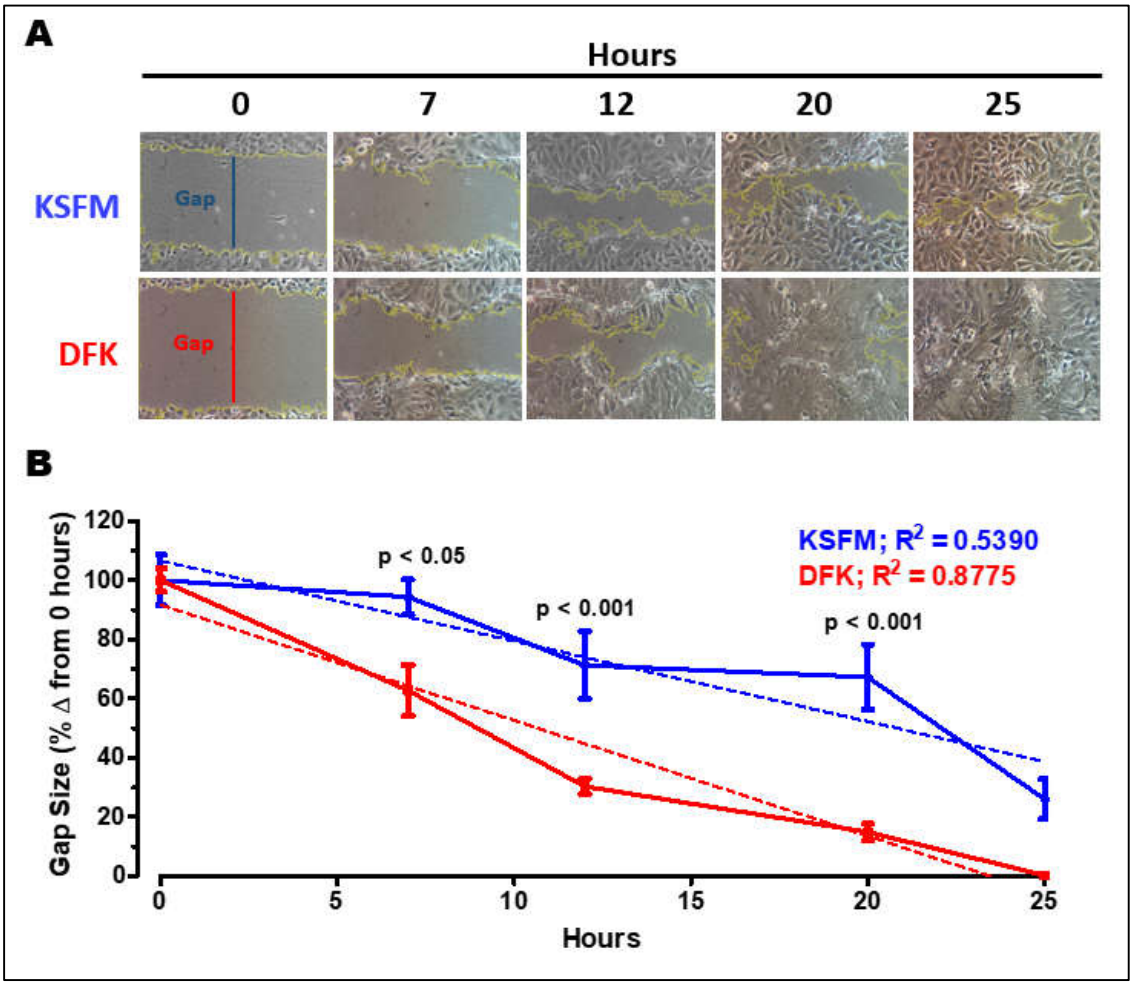

Figure 6. Wound healing assay of OKF6/TERT-2 cells growing in KSFM or DFK. The gap, labeled at 0 hours, indicates a representative width of the initial wounds (A). ImageJ was used to measure the gap closure over time. Each time-point represents the mean ± SE of the gap width as a percentage of the initial size, where n = 4. Dashed lines indicate linear regressions. Significance between KSFM and DFK at each time-point is indicated by the p values (B).

2.7. Effects of E-liquids ± flavors on OKF6/TERT cells after DFK and KSFM culturing

Protein content and cellular viability were assessed on cell cultures in both media after exposure to 1% E-liquids ± flavors (v/v) for 24 hours. Figure 7 shows roughly the same protein levels in most conditions in both media. Tobacco and menthol conditions show a significantly higher level of proteins from DFK cultures ($p < 0.05$). The addition of 1% E-liquids ± flavors do not alter the total protein content in KSFM cultures with respect to those of untreated KSFM cultures. However, protein content is significantly altered after exposure to 1% E-liquid + cinnamon flavor in DFK cultures ($p < 0.001$) (Fig 7A). Figure 7B shows the total number of viable cells in DFK or KSFM cultures after adding 1% E-liquids ± flavors for 24 hours. Regardless of treatments, there is a significant disparity of viable cell numbers between DFK and KSFM cultures ($p < 0.05$), confirming the results in Figure 2. Cinnamon flavor significantly reduces the number of viable cells in both DFK and KSFM cultures. Lastly, menthol, strawberry and blueberry flavors also significantly reduce the total number of viable cells in DFK cultures ($P < 0.01$), but this trend is not observed in KSFM cultures. In general, these results indicate that OKF6/TERT-2 cells grown in DFK are more sensitive to the effects of E-liquids with flavors. Fig 7C shows the total levels of lactate dehydrogenase (LDH) activity in the supernatant of treated cells as a percentage of completely lysed cells. Interestingly, in every case, the highest level of LDH activity is roughly 6%, which means that a significant but modest amount of LDH is

Preprints (www.preprints.org) | NOT PEER-REVIEWED | Posted: 9 January 2023 doi:10.20944/preprints202301.0150.v1

leaking out of cells treated with E-liquid with menthol and cinnamon. There is no significant difference in LDH activity between KSFM and DFK cultures within the same treatments. Although the viability data (Fig 7B) and the LDH activity data (Fig 7C) appear to be counterintuitive, a potential explanation is that E-liquid treatments induce cells to undergo apoptosis, where cytoplasmic contents, including LDH, are packaged within apoptotic bodies and not released to the supernatant. Furthermore, Fig 7A shows that the overall protein content is still present in the samples supporting the possibility of the existence of apoptotic bodies.

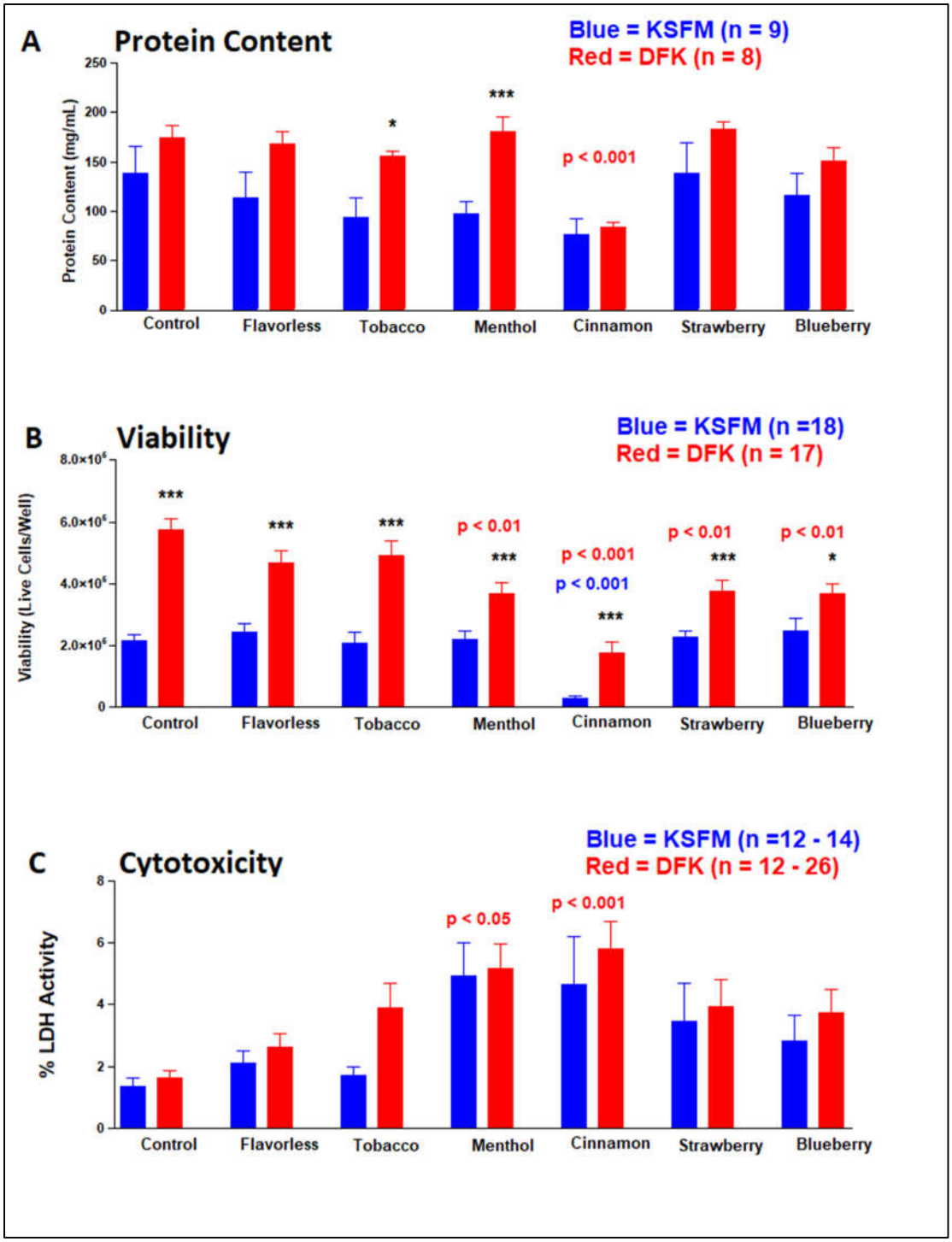

Figure 7. Effects of E-liquids ± flavors on OKF6/TERT-2 cells growing in KSFM or DFK. Total protein content (A), cellular viability (B), and cytotoxicity (C) were measured, and each bar indicates their means ± SE. * = $p < 0.05$ and *** = $p < 0.001$ when comparing KSFM vs DFK within each treatment.

Preprints (www.preprints.org) | NOT PEER-REVIEWED | Posted: 9 January 2023 doi:10.20944/preprints202301.0150.v1

The p values in blue and red signify statistical significance between control and treatment groups for either KSFM or DFK, respectively.

3. Discussion

The present study provides evidence that the OKF6/TERT-2 cell line grown in DFK, a novel medium composed of a 1:1 mixture of KSFM and DMEM/F-12, confers comparable morphology, mucin production, as well as *ZO-1* and *occludin* gene expression. However, monolayer growth, *claudin-1* expression, and wound healing ability occur at elevated levels in cells grown in DFK. In addition, OKF6/TERT-2 cells display a pronounced sensitivity to E-liquids ± flavors.

Confocal microscopy with 3D imaging of OKF6/TERT-2 monolayers showed similar morphology of monolayers on both media. However, cells in the DFK medium yielded rapid proliferation without significant alterations to actin filament arrangement (Fig 3A). Both media led to the formation of small cell aggregates within 2 days, however the coalescence of these aggregates occurred 24 hours sooner when cells were grown on DFK (Fig 2A). Regarding other oral epithelial cell lines, investigators have found that telomerase immortalized gingival keratinocytes (TIGKs) demonstrate a characteristic 'cobblestone' appearance 2-3 days after seeding [53], which is similarly observed in OKF6/TERT-2 cells (Fig 1 and Fig 2A) and other oral epithelial cell lines grown in KSFM [54], as well as *ex vivo* oral mucosal epithelial cells grown in culture [55]. Our results indicate this cellular morphology remains unchanged in DFK and KSFM media and is consistent with the squamous morphology seen in the human oral cavity [56–58].

The increased cell density in DFK is the result of increased propensity for rapid proliferation and smaller cell size (Fig 3). Unlike TIGK cells, which rarely reach 100% confluence in KSFM containing 0.04 mM calcium [53], the present study suggests that OKF6/TERT-2 cells grow more rapidly in the DFK composite medium containing 0.4 mM calcium (Fig 2). It has generally been accepted that higher cytosolic calcium levels correlate with increased cellular differentiation progressing from the proliferative basal layer to the superficial non-proliferative stratum corneum *in vivo* [59–62]. However, the biochemistry behind this process has been complicated by more recent reports of basal layer cells actually containing relatively lower calcium content [63]. Possibly, the higher calcium in both KSFM and DFK could promote a proliferative phenotype in OKF6/TERT-2 cells, displaying gene expression and function (Fig 4-6), but when cells reach confluence and contact inhibition, they show a more non-proliferative phenotype. Moreover, DFK seems to enhance the transition from proliferative to non-proliferative states.

The expression and function of tight junction proteins are critical for epithelial cells from a range of anatomic sites, including the oral epithelium, to maintain a clear barrier between the outside environment and the sub-epithelial tissues. For example, there is a positive correlation between the expression of *claudin-1* and *occludin* with proliferation and migration to close wounds [64]. Since *claudin-1* is overexpressed in OKF6/TERT-2 cells cultured in DFK (Fig 4B) this could potentially support the faster recovery of the wound in this medium (Fig 7).

To remain an appropriate model for research on the oral epithelia, OKF6/TERT-2 cells should demonstrate a comparable expression of tight junctions in any media selected, which was observed in our experiments with both media tested. Our results indicate that *occludin* and *ZO-1* are similarly expressed (Fig 4). This correlates with other studies where tight junction genes are well expressed, and even overexpressed when challenged. For example, exposure to the commensal organism, *Streptococcus gordonii*, leads to elevated expression of the tight junctions *ZO-1*, *ZO-2* and *JAM-A*, increasing the paracellular barrier function [65]. On the other hand, oral pathogens, such as *Porphyromonas gingivalis*, alter the expression levels of tight junctions [66–68], which ultimately leads to disease. This alteration in barrier integrity is correlated to susceptibility to severe allergic reactions [69], and permeability of surfaces in many other anatomic sites, notably the intestinal mucosa [70]. Further studies should focus on the role of tight junction genes in the presence of invasive oral bacteria.

Preprints (www.preprints.org) | NOT PEER-REVIEWED | Posted: 9 January 2023 doi:10.20944/preprints202301.0150.v1

MUC1 and MUC4 were found to be similarly expressed when cells were cultured in KSFM and DFK (Fig 4A), indicating that both media are effective in maintaining this phenotype in OKF6/TERT-2 cells. MUC1 is broadly expressed in mucosal tissues [71]. Similarly, mucins are released by OKF6/TERT-2 cells during culture and later found in the supernatant (Fig 5). This is consistent with other findings indicating that membrane-associated mucins are released into solution [72–74], which in the case of the oral cavity, become part of saliva. Mucins also function as decoys for the clearance of microbial infections. For example, MUC1 binds to adenovirus, reducing infection into host cells [75], where the virus binds to O-linked carbohydrates on the mucin [76]. In addition, MUC1 also binds to bacteria, including *Pseudomonas aeruginosa* [77], and *Helicobacter pylori* [78]. Furthermore, mucins could serve as a source of carbohydrates for commensal species, such as *Streptococcus gordonii* catabolism [79] or as decoys for clearance of cariogenic *Streptococcus mutans* [80,81], indicating a role in the maintenance and homeostasis of the oral microenvironment. Since both DFK and KSFM support the expression and release of mucins in OKF6/TERT-2 cells, similar to *in vivo* oral epithelial cells, either media could be used for further studies in mucin expression and function.

Based on linear regression, results of wound-healing assays demonstrate that OKF6/TERT-2 cells recover within 24 hours in DFK and by 39 hours in KSFM (Fig 6). Other wound-healing studies with the same cell line used media containing FBS. For example, OKF6/TERT-2 cells cultured with KSFM + 1% FBS recover nearly 100% by 18 hours [82]. In addition, the same cell line, cultured in Roswell Park Medical Institute (RPMI) medium + 10% FBS recovered by 24 hours after onset of the scratch in the wound-healing assay [83]. In a study by Shaikh et al., using DMEM/F12 + 10% FBS, full recovery of OKF6/TERT-2 cells took over three days [84]. This study demonstrates that cell growth with DMEM/F12 alone, even when supplied with FBS, is not as effective as KSFM or DFK. Our protocol includes a mixture of DMEM/F12 and KSFM, which results in a set of nutrients that yield faster growth and wound-healing recovery compared to DMEM/F12 alone. Shaikh and coworkers [84] also tested the effects of E-liquids on OKF6/TERT-2 cells and reported a decrease in viability after treatments, which agree with our results in figure 7B. Alanazi et al. [85] show that the pathogenesis of yeast *Candida albicans* on a human gingival epithelial carcinoma cell line (grown in RPMI + 10% FBS) is increased after the microbe is exposed to tobacco flavored aerosol. While many studies make use of media + FBS, few studies used serum-free media. For example, Catalá-Valentín and coworkers [86] grew OKF6/TERT-2 cells in KSFM, using a protocol like ours, and treated cariogenic *S. mutans* with electronic cigarette aerosol containing menthol and nicotine. Subsequently, researchers found that *S. mutans* adherence to OKF6/TERT-2 cells increases after aerosol treatments. Furthermore, a parallel study by Catalá-Valentín et al. [87] shows OKF6/TERT-2 immunosuppression, where cytokine expression of the cells, challenged with *Staphylococcus aureus*, is significantly decreased after exposure to flavorless electronic cigarette aerosol. Future studies from our group aim to dissect the effects of E-liquids on the oral mucosa, specifically on (1) the cellular and molecular biology, including changes in gene expression and wound healing; (2) the physiological stress response, including glutathione and cytokine alterations; and (3) the host-bacteria interactions using both commensal and pathogenic oral species.

In the present study, a monolayer culturing technique was used to compare the effects of a novel culture medium on the OKF6/TERT-2 cell line illustrating that DFK is a viable alternative medium, and more importantly, showing that this oral epithelial cell line remains an appropriate model of oral physiology during multiple conditions. Recently, organotypic 3-dimensional cultures with multiple cell layers have been developed to reflect the oral environment more accurately and therefore increase the pertinence of *in vitro* experimentation [88–91], which is a limitation of this investigation. This study was conducted on the premise that a novel culture medium should be evaluated on a monolayer before extension to 3D models. Additionally, using a single cell line for the evaluation of this novel DFK medium is another limitation. Future studies should explore additional oral cell lines, such as gingival epithelial cells, in DFK or other media to further

 doi:10.20944/preprints202301.0150.v1

expand *in vitro* oral epithelial models. In addition, expression levels of only five genes were measured. These genes were chosen because they are involved in the maintaining integrity of the oral epithelia. In prospective studies, other genes and gene products should be analyzed.

The oral cavity is frequently the first site of exposure to external insults. Therefore, a biologically representative model of the oral environment, such as the one described in this study, is essential considering the vast array of pathophysiological conditions that may occur in the mouth. For example, the oral epithelium was recently identified to contain angiotensin converting enzyme-2 (ACE2) [92], a receptor for the spike protein on severe acute respiratory syndrome coronavirus-2 (SARS CoV2). A recent study reports the use of chewing gum containing ACE2 decoy proteins protecting the host from microbial infection [93]. Consequently, DFK may facilitate research in such host-pathogen studies. Since our research interests focus on the use of electronic cigarettes and the effects of these on oral mucosa, this study compared the applicability of DFK and KSFM on OKF6/TERT2 cultures exposed to E-liquids ± flavors. An oral epithelial cell line, amenable to multiple culture conditions, without compromising the phenotype of the model, will not only facilitate further research in these areas using monolayer culturing techniques but also provide a basis for further improved organotypic 3D cultures.

Based on the results of these experiments, KSFM is essential to seed the OKF6/TERT-2 cell line. However continued growth of the cultures could be achieved by either keeping the cells in KSFM or switching to DFK. The latter yielded faster growth and more dense cultures, which appear to enhance the wound healing process and the expression of *claudin-1*. In addition, the use of DFK rendered the cells more sensitive to the effects of E-liquids ± flavors. Switching to DFK is a more favorable protocol because of the benefit of decreased culturing time, thus expediting research efforts.

4. Materials and Methods

4.1. Culture media

All culture media reagents and supplies were purchased from ThermoFisher Scientific (Waltham, MA, USA) unless otherwise indicated. KSFM was prepared by adding 30 µg/mL bovine pituitary extract, 1 ng/mL epithelial growth factor, 1 mM glutamine, 0.3 mM calcium chloride and 100 U/mL penicillin/streptomycin as previously described [7]. DMEM/F12 was prepared by adding the same reagents at the same concentrations as KSFM. DFK was prepared by mixing prepared DMEM/F12 and prepared KSFM at a 1:1 (v/v). All media were stored at 4 °C.

4.2. Cell culture, morphology and growth

OKF6/TERT-2 cells were kindly provided by Dr. Gill Diamond at Louisville University School of Dentistry, but were originally established in the study by Dickson et al. [1]. Cells were cultured first in KSFM and then passaged onto experiments in either of KSFM and/or DFK. For all experiments, cells were seeded at 52,000 cells/cm^2 and cultured at 37 °C 5% CO_2, changing the media within the first 24 hours and then every 2 or 3 days until confluent. To evaluate initial cell morphology and growth, OKF6/TERT-2 cells were seeded in 24-well plates at 100,000 cells/well and grown in either KSFM or DFK. In latter experiments, cells were seeded in KSFM, cultured for 24 hours, spent media were removed and replaced with either fresh KSFM or DFK. Cells were imaged at 100× magnification using a Nikon Eclipse TE2000-U inverted microscope equipped with a Nikon Digital Sight DS-Fi1 camera and NIS Elements Imagine Software (Nikon Instruments Inc, Melvin, NY, USA). For each type of media, four wells were trypsinized and counted every 24 hours using the trypan blue exclusion assay with the hemocytometer and light microscopy.

Preprints (www.preprints.org) | NOT PEER-REVIEWED | Posted: 9 January 2023 doi:10.20944/preprints202301.0150.v1

4.3. Confocal Microscopy

To further evaluate cellular morphology, OKF6/TERT-2 cells were seeded in chamber slides and grown to confluency in KSFM or DFK media for four days. Then, monolayers were washed in PBS and fixed in 4% paraformaldehyde for 20 minutes, followed by PBS washes and aldehyde quenching using 0.1% glycine. Permeabilization was performed with 0.1% Triton X-100 in PBS for 15 minutes followed by washes and blocking with 1% bovine serum albumin in PBS. Phalloidin-FITC conjugate at 5 µg/mL in PBS was added for 30 minutes to stain F-actin (green). Samples were then washed 3 times with PBS and mounting media containing DAPI were added to stain the cell nucleus (blue). Cell samples were observed under a Carl Zeiss LSM880 laser scanning confocal microscope (Carl Zeiss Inc. White Plains, NY) at 630× magnification with oil immersion using an excitation wavelength of 405 nm and 488 nm for DAPI and FITC, respectively. Z-stacks (height) were acquired at slow speed and high resolution with an optical slicing of 1 µm. The ZEN 3.5 software (Carl Zeiss Inc. White Plains, NY, USA) was used to obtain 3D images. The confocal microscope and software were accessed in the Biological Sciences Department at the College of Arts and Sciences, Lehigh University (Bethlehem, PA, USA). The average number of cells per field view was achieved by counting the number of nuclei (blue) in both KSFM and DFK (n = 8). To calculate the average area of cells, the total area of the field of view (135 µm x 135 µm) was divided by the average number of cells. The average height of the cultures in both media was calculated by averaging the number of slices (each slice = 1 µm) in all Z-stacks (n = 17 for KSFM and n = 18 for DFK). The cell volume was calculated by multiplying the cell area by the average height.

4.4. Expression of mucins and tight junction genes

OKF6/TERT-2 cells were seeded and grown to confluency in 6-well plates using either KSFM or DFK. Once 100% confluent, media were collected and stored. Monolayers were washed twice with PBS to remove excess cellular debris and RNA was collected with the mirVana miRNA isolation kit, 100% ethanol and phenol:chloroform, following the manufacturer's instructions. The RNA concentration was determined with the nanodrop, and the VILO reverse transcription kit was used to obtain cDNA. *β-actin, claudin-1, occludin, zonula occluden* (ZO-1), *muc1* and *muc4* were amplified with TaqMan primers. Cycle threshold (Ct) values were obtained using the QuantStudio 3 qPCR cycler (Applied Biosystems, Waltham, MA, USA), and $2^{-\Delta\Delta Ct}$ values were calculated using *β-actin* as control. Data are presented as percentages of *β-actin* expression levels.

4.5. SDS-PAGE for released glycoproteins

Human saliva was collected from five healthy individuals under IRB approval code Cuadra_S19_18. Saliva samples were pooled and sterilized following a previously established protocol [44]. Approximately 12 mL of OKF6/TERT-2 cell culture supernatants in KSFM and DFK from two separate experiments were filtered through Amicon Ultra 30K centrifugal filters. The concentrates were resuspended in sterile water to dilute the salts and re-filtered. In addition, fresh KSFM and DFK media, as well as sterile human saliva, were also filter-concentrated. After Amicon filtration, all samples contain macromolecules above 30 kiloDaltons (kD), and protein concentrations were determined with the Micro BCA Protein Assay Kit, following manufacturer's instructions. Samples were adjusted to equal protein concentrations and 30 µg of proteins were separated by SDS-PAGE. Then, all heavily glycosylated glycoproteins were stained using the PAS protocol [80,94]. After obtaining the image of all glycoproteins present in the gel, Coomassie blue was used to stain the rest of the proteins in the samples and the gel was imaged again.

4.6. Wound/Healing assay

OKF6/TERT-2 cells were seeded and grown to confluency in 6-well plates or 35 mm tissue culture dishes (same size) using either KSFM or DFK. Once 100% confluent, media

Preprints (www.preprints.org) | NOT PEER-REVIEWED | Posted: 9 January 2023 doi:10.20944/preprints202301.0150.v1

were removed, and using a sterile 1 mL pipet tip, a scratch (a straight line across the diameter of the well or dish) was made in all cultures. Monolayers were washed twice with PBS to remove excess cellular debris and new media were added to all cultures. Scratched monolayers were immediately imaged at 100× magnification using a Nikon Eclipse TE2000-U inverted microscope as indicated above and cultures were incubated at 37 °C 5% CO_2 for one day. To assess wound recovery, cultures were imaged at 0, 7, 12 and 20 hours after scratching.

To quantify and compare the rate of OKF6/TERT-2 wound-heal recovery across both KSFM and DFK, the computer image processing program ImageJ with the open source *Wound Healing Size Tool* (WHST) plugin optimized for *in-vitro* wound-heal assay analysis was utilized [95,96]. The WHST supports accurate discrimination between cell monolayer and open wound area by fixing a line dividing the two regions, driven both by its independent algorithmic analysis as well as user-defined input of variance filter radius values and manual modification of saturation percentage in contrast enhancement. Open wound area was defined by pixel area (pixels^2) and was quantified using WHST analysis of the imaged monolayers over time.

4.7. Effects of E-liquid treatments: protein concentration, viability and cytotoxicity

E-liquids were prepared as previously described [44,45]. Briefly, the flavorless E-liquid mixture was prepared by mixing equal volumes of propylene glycol and vegetable glycerine and supplemented with 20 mg/mL nicotine. In addition, flavors including tobacco, menthol, cinnamon, strawberry, and blueberry, were added to a final volume of 5% (v/v) to flavorless E-liquid. All E-liquids ± flavors and their components were stored at 4°C or at room temperature, respectively.

To test the effects of E-liquids on OKF6/TERT-2 cells, confluent cultures in DFK or KSFM were exposed 1% E-liquids (v/v) dissolved in either media. Confluent monolayers were exposed to these E-liquid treatments at 37°C, 5% CO_2 for 24 hours. Supernatants were removed and stored at -20 °C for LDH cytotoxicity assays. Cells were trypsinized, diluted to a final volume of 1 mL and from the resulting cell suspension, only 10 µL were used for cell viability via trypan blue exclusion. The remaining cells were pelleted and stored at -20 °C. Cell pellets were lysed in a final volume of 1 mL 0.2% Triton-X 100 solution, syringe-filtered (0.22 µm), and assayed for total protein, as indicated above (section 4.6). The LDH cytotoxicity assay kit was used to perform cytotoxicity assays according to manufacturer's instructions. Briefly, untreated cell monolayers were lysed with lysis buffer (provided in the kit) and used as reference for 100% LDH activity. Supernatants were thawed and 50 µL were added to 50 µL of the reaction mixture and allowed to incubate for 30 minutes in the dark at room temperature. Finally, 50 µL of stopping solution was added to all reactions and absorbance was read at 595 nm.

4.8. Statistical analysis

Means and standard errors of the mean (SE) were calculated and analyzed for all quantitative experiments. Two-way ANOVA followed by Bonferroni post-hoc analysis was used to compare the effects of DFK vs KSFM on the viability and wound healing ability of OKF6/TERT-2 cells over time. Additionally, linear regression analyses and correlation coefficients for wound-healing assays were performed over time and extrapolated to the x-intercept. Student's t-test was used to compare the effects of DFK vs KSFM on the height of OKF6/TERT-2 cells (based Z-stacks where each optical slice is 1 µm) and the expression of mucin and tight junction genes. For comparison of protein content and viability of OKF6/TERT-2 cells grown in DFK or KSFM in the presence of E-liquid ± flavors, a one-way ANOVA followed by Bonferroni post-hoc analysis was used to determine statistical significance between treatment groups within the same media and a student's t-test was used to determine statistical significance between media for each treatment group. All statistical tests were performed using GraphPad Prism® version 5.02

(GraphPad Software, San Diego, CA, USA). For all tests, $p < 0.05$ was considered statistically significant.

Author Contributions: Conceptualization, G.A. and D.P.; methodology, G.A., A.S., R.S., J.M., D.P.; software, G.A., R.S. and D.P.; investigation, G.A., A.S., R.S., J.M., D.P.; validation, G.A. and D.P.; formal analysis, G.A., A.S., R.S., J.M. and D.P.; writing—original draft preparation, G.A. and A.S.; writing—G.A., A.S. and D.P.; project administration, G.A. and D.P.; funding acquisition, G.A. and D.P. All authors have read and agreed to the published version of the manuscript.

Funding: This research was supported by funding derived from the Rising Scholar's Award granted to Giancarlo Cuadra by the Office of the Provost at Muhlenberg College.

Institutional Review Board Statement: The study was conducted in accordance with the Declaration of Helsinki, and approved by the Institutional Review Board (or Ethics Committee) of Muhlenberg College (Cuadra_S19_18 from May 13th 2019).

Informed Consent Statement: Verbal informed consent was obtained from all subjects involved in the study.

Data Availability Statement: The contributions presented in the study are included in the publication or can be located through the section entitled Supplementary Material. Any further questions or inquiries can be directed to the corresponding author.

Acknowledgments: Authors would like to thank Marten Edwards and Bruce Wightman from Muhlenberg College for their review of the manuscript. In addition, authors are grateful for Lee Graham at Lehigh University for his technical assistance with confocal microscopy.

Conflicts of Interest: The authors declare no conflict of interest.

References

1. Dickson, M.A.; Hahn, W.C.; Ino, Y.; Ronfard, V.; Wu, J.Y.; Weinberg, R.A.; Louis, D.N.; Li, F.P.; Rheinwald, J.G. Human Keratinocytes That Express HTERT and Also Bypass a P16(INK4a)-Enforced Mechanism That Limits Life Span Become Immortal yet Retain Normal Growth and Differentiation Characteristics. *Mol Cell Biol* **2000**, *20*, 1436–1447, doi:10.1128/MCB.20.4.1436-1447.2000.
2. Reyes, J.D. Intestinal Transplantation: An Unexpected Journey. Robert E. Gross Lecture. *J Pediatr Surg* **2014**, *49*, 13–18, doi:10.1016/j.jpedsurg.2013.09.022.
3. Trachootham, D.; Chingsuwanrote, P.; Yoosadiang, P.; Mekkriangkrai, D.; Ratchawong, T.; Buraphacheep, N.; Kijanukul, S.; Saekhow, S.; Pongpitchayadej, O.; Vongvachvasin, K.; et al. Partial Substitution of Glucose with Xylitol Suppressed the Glycolysis and Selectively Inhibited the Proliferation of Oral Cancer Cells. *Nutr Cancer* **2017**, *69*, 862–872, doi:10.1080/01635581.2017.1339097.
4. Goessel, G.; Quante, M.; Hahn, W.C.; Harada, H.; Heeg, S.; Suliman, Y.; Doebele, M.; von Werder, A.; Fulda, C.; Nakagawa, H.; et al. Creating Oral Squamous Cancer Cells: A Cellular Model of Oral–Esophageal Carcinogenesis. *Proc Natl Acad Sci U S A* **2005**, *102*, 15599–15604, doi:10.1073/pnas.0409730102.
5. Alekseev, O.; Donegan, W.E.; Donovan, K.R.; Limonnik, V.; Azizkhan-Clifford, J. HSV-1 Hijacks the Host DNA Damage Response in Corneal Epithelial Cells through ICP4-Mediated Activation of ATM. *Invest Ophthalmol Vis Sci* **2020**, *61*, 39, doi:10.1167/iovs.61.6.39.
6. Chen, W.; Alshaikh, A.; Kim, S.; Kim, J.; Chun, C.; Mehrazarin, S.; Lee, J.; Lux, R.; Kim, R.H.; Shin, K.H.; et al. Porphyromonas Gingivalis Impairs Oral Epithelial Barrier through Targeting GRHL2. *J Dent Res* **2019**, *98*, 1150–1158, doi:10.1177/0022034519865184.
7. Hanel, A.N.; Herzog, H.M.; James, M.G.; Cuadra, G.A. Effects of Oral Commensal Streptococci on Porphyromonas Gingivalis Invasion into Oral Epithelial Cells. *Dent J (Basel)* **2020**, *8*, doi:10.3390/dj8020039.
8. Rajagopalan, P.; Patel, K.; Jain, A.P.; Nanjappa, V.; Datta, K.K.; Subbannayya, T.; Mangalaparthi, K.K.; Kumari, A.; Manoharan, M.; Coral, K.; et al. Molecular Alterations Associated with Chronic Exposure to Cigarette Smoke and Chewing Tobacco in Normal Oral Keratinocytes. *Cancer Biol Ther* **2018**, *19*, 773–785, doi:10.1080/15384047.2018.1470724.
9. Patil, S.; Patel, K.; Advani, J.; Subbannayya, T.; Rajagopalan, P.; Babu, N.; Solanki, H.; Bhandi, S.; Sidransky, D.; Chatterjee, A.; et al. Multiomic Analysis of Oral Keratinocytes Chronically Exposed to Shisha. *J Oral Pathol Med* **2019**, *48*, 284–289, doi:10.1111/jop.12828.
10. Nanjappa, V.; Renuse, S.; Sathe, G.J.; Raja, R.; Syed, N.; Radhakrishnan, A.; Subbannayya, T.; Patil, A.; Marimuthu, A.; Sahasrabuddhe, N.A.; et al. Chronic Exposure to Chewing Tobacco Selects for Overexpression of Stearoyl-CoA Desaturase in Normal Oral Keratinocytes. *Cancer Biol Ther* **2015**, *16*, 1593–1603, doi:10.1080/15384047.2015.1078022.

11. Li, W.-C.; Ralphs, K.L.; Slack, J.M.W.; Tosh, D. Keratinocyte Serum-Free Medium Maintains Long-Term Liver Gene Expression and Function in Cultured Rat Hepatocytes by Preventing the Loss of Liver-Enriched Transcription Factors. *Int J Biochem Cell Biol* **2007**, *39*, 541–554, doi:10.1016/j.biocel.2006.10.017.
12. Cross, W.R.; Eardley, I.; Leese, H.J.; Southgate, J. A Biomimetic Tissue from Cultured Normal Human Urothelial Cells: Analysis of Physiological Function. *American Journal of Physiology-Renal Physiology* **2005**, *289*, F459–F468, doi:10.1152/ajprenal.00040.2005.
13. Hu, L.; Pu, Q.; Zhang, Y.; Ma, Q.; Li, G.; Li, X. Expansion and Maintenance of Primary Corneal Epithelial Stem/Progenitor Cells by Inhibition of TGFβ Receptor I-Mediated Signaling. *Exp Eye Res* **2019**, *182*, 44–56, doi:10.1016/j.exer.2019.03.014.
14. Perduns, R.; Volk, J.; Plum, M.; Gutzki, F.; Kaever, V.; Geurtsen, W. Effects of HEMA on Nrf2-Related Gene Expression Using a Newly Developed 3D Co-Culture Model of the Oral Mucosa. *Dental Materials* **2019**, *35*, 1214–1226, doi:10.1016/j.dental.2019.05.006.
15. Reyes, M.; Peña-Oyarzún, D.; Silva, P.; Venegas, S.; Criollo, A.; Torres, V.A. Nuclear Accumulation of β-Catenin Is Associated with Endosomal Sequestration of the Destruction Complex and Increased Activation of Rab5 in Oral Dysplasia. *FASEB J* **2020**, *34*, 4009–4025, doi:10.1096/fj.201902345RR.
16. Yiannis, C.; Huang, K.; Tran, A.N.; Zeng, C.; Dao, E.; Baselyous, O.; Mithwani, M.A.; Paolini, R.; Cirillo, N.; Yap, T.; et al. Protective Effect of Kava Constituents in an in Vitro Model of Oral Mucositis. *J Cancer Res Clin Oncol* **2020**, *146*, 1801–1811, doi:10.1007/s00432-020-03253-3.
17. Millhouse, E.; Jose, A.; Sherry, L.; Lappin, D.F.; Patel, N.; Middleton, A.M.; Pratten, J.; Culshaw, S.; Ramage, G. Development of an in Vitro Periodontal Biofilm Model for Assessing Antimicrobial and Host Modulatory Effects of Bioactive Molecules. *BMC Oral Health* **2014**, *14*, 80, doi:10.1186/1472-6831-14-80.
18. Villar, C.C.; Lin, A.L.; Cao, Z.; Zhao, X.-R.; Wu, L.-A.; Chen, S.; Sun, Y.; Yeh, C.-K. Anticandidal Activity and Biocompatibility of a Rechargeable Antifungal Denture Material. *Oral Dis* **2013**, *19*, 287–295, doi:10.1111/odi.12000.
19. Volk, J.; Leyhausen, G.; Geurtsen, W. Glutathione Level and Genotoxicity in Human Oral Keratinocytes Exposed to TEGDMA. *J Biomed Mater Res B Appl Biomater* **2012**, *100*, 391–399, doi:10.1002/jbm.b.31960.
20. Volk, J.; Leyhausen, G.; Wessels, M.; Geurtsen, W. Reduced Glutathione Prevents Camphorquinone-Induced Apoptosis in Human Oral Keratinocytes. *Dental Materials* **2014**, *30*, 215–226, doi:10.1016/j.dental.2013.11.008.
21. Wessels, M.; Rimkus, J.; Leyhausen, G.; Volk, J.; Geurtsen, W. Genotoxic Effects of Camphorquinone and DMT on Human Oral and Intestinal Cells. *Dental Materials* **2015**, *31*, 1159–1168, doi:10.1016/j.dental.2015.06.007.
22. DMEM - Dulbecco's Modified Eagle Medium - US Available online: //www.thermofisher.com/us/en/home/life-science/cell-culture/mammalian-cell-culture/classical-media/dmem.html (accessed on 8 January 2022).
23. Almela, T.; Brook, I.M.; Moharamzadeh, K. Development of Three-Dimensional Tissue Engineered Bone-Oral Mucosal Composite Models. *J Mater Sci Mater Med* **2016**, *27*, 65, doi:10.1007/s10856-016-5676-7.
24. Barker, E.; AlQobaly, L.; Shaikh, Z.; Franklin, K.; Moharamzadeh, K. Implant Soft-Tissue Attachment Using 3D Oral Mucosal Models—A Pilot Study. *Dent J (Basel)* **2020**, *8*, 72, doi:10.3390/dj8030072.
25. Basso, F.G.; Cardoso, L.M.; Ribeiro, I.M.; Rizzi, E.; Pansani, T.N.; Hebling, J.; de Souza Costa, C.A. Influence of Bisphosphonates on Oral Implantology: Sodium Alendronate and Zoledronic Acid Enhance the Synthesis and Activity of Matrix Metalloproteinases by Gingival Fibroblasts Seeded on Titanium. *Arch Oral Biol* **2021**, *127*, 105134, doi:10.1016/j.archoralbio.2021.105134.
26. Ravosa, M.J.; Ning, J.; Liu, Y.; Stack, M.S. Bisphosphonate Effects on the Behaviour of Oral Epithelial Cells and Oral Fibroblasts. *Arch Oral Biol* **2011**, *56*, 491–498, doi:10.1016/j.archoralbio.2010.11.003.
27. Fageeh, H.N.; Bhandi, S.; Mashyakhy, M.; Kahtani, A.A.; Badran, Z.; Mehta, D.; Fageeh, H.I.; Balaji, T.M.; Baeshen, H.A.; Varadarajan, S.; et al. Viability of Quercetin-Induced Dental Pulp Stem Cells in Forming Living Cellular Constructs for Soft Tissue Augmentation. *J Pers Med* **2021**, *11*, 430, doi:10.3390/jpm11050430.
28. Omata, Y.; Lewis, J.B.; Rotenberg, S.; Lockwood, P.E.; Messer, R.L.W.; Noda, M.; Hsu, S.D.; Sano, H.; Wataha, J.C. Intra- and Extracellular Reactive Oxygen Species Generated by Blue Light. *J Biomed Mater Res A* **2006**, *77*, 470–477, doi:10.1002/jbm.a.30663.
29. Furuse, M.; Takai, Y. Recent Advances in Understanding Tight Junctions. *Fac Rev* **2021**, *10*, 18, doi:10.12703/r/10-18.
30. Anderson, J.M. Molecular Structure of Tight Junctions and Their Role in Epithelial Transport. *News Physiol Sci* **2001**, *16*, 126–130, doi:10.1152/physiologyonline.2001.16.3.126.
31. Dawes, C. Salivary Flow Patterns and the Health of Hard and Soft Oral Tissues. *J Am Dent Assoc* **2008**, *139 Suppl*, 18S-24S, doi:10.14219/jada.archive.2008.0351.
32. Bansil, R.; Turner, B.S. Mucin Structure, Aggregation, Physiological Functions and Biomedical Applications. *Current Opinion in Colloid & Interface Science* **2006**, *11*, 164–170, doi:10.1016/j.cocis.2005.11.001.
33. CREETH, J.M. CONSTITUENTS OF MUCUS AND THEIR SEPARATION. *British Medical Bulletin* **1978**, *34*, 17–24, doi:10.1093/oxfordjournals.bmb.a071454.
34. Rose, M.C.; Voynow, J.A. Respiratory Tract Mucin Genes and Mucin Glycoproteins in Health and Disease. *Physiological Reviews* **2006**, *86*, 245–278, doi:10.1152/physrev.00010.2005.
35. Grondin, J.A.; Kwon, Y.H.; Far, P.M.; Haq, S.; Khan, W.I. Mucins in Intestinal Mucosal Defense and Inflammation: Learning From Clinical and Experimental Studies. *Frontiers in Immunology* **2020**, *11*.
36. Ueta, E.; Tanida, T.; Doi, S.; Osaki, T. Regulation of Candida Albicans Growth and Adhesion by Saliva. *J Lab Clin Med* **2000**, *136*, 66–73, doi:10.1067/mlc.2000.107304.
37. Leone, C.W.; Oppenheim, F.G. Physical and Chemical Aspects of Saliva as Indicators of Risk for Dental Caries in Humans. *J Dent Educ* **2001**, *65*, 1054–1062.

38. Gendler, S.J.; Spicer, A.P.; Lalani, E.N.; Duhig, T.; Peat, N.; Burchell, J.; Pemberton, L.; Boshell, M.; Taylor-Papadimitriou, J. Structure and Biology of a Carcinoma-Associated Mucin, MUC1. *Am Rev Respir Dis* **1991**, *144*, S42-47, doi:10.1164/ajrccm/144.3_pt_2.S42.
39. Gum, J.R. Mucin Genes and the Proteins They Encode: Structure, Diversity, and Regulation. *Am J Respir Cell Mol Biol* **1992**, *7*, 557–564, doi:10.1165/ajrcmb/7.6.557.
40. Sen, S.; Sharma, S.; Gupta, A.; Gupta, N.; Singh, H.; Roychoudhury, A.; Mohanty, S.; Sen, S.; Nag, T.C.; Tandon, R. Molecular Characterization of Explant Cultured Human Oral Mucosal Epithelial Cells. *Invest Ophthalmol Vis Sci* **2011**, *52*, 9548–9554, doi:10.1167/iovs.11-7946.
41. Supruniuk, K.; Czarnomysy, R.; Muszyńska, A.; Radziejewska, I. Anti-Cancer Effects of Pyrazole-Platinum(II) Complexes Combined with Anti-MUC1 Monoclonal Antibody versus Monotherapy in DLD-1 and HT-29 Colon Cancer Cells. *Transl Oncol* **2022**, *18*, 101348, doi:10.1016/j.tranon.2022.101348.
42. Abdelwhab, A.; Shaker, O.; Aggour, R.L. Expression of Mucin1 in Saliva in Oral Squamous Cell Carcinoma and Oral Potentially Malignant Disorders (Case Control Study). *Oral Dis* **2022**, doi:10.1111/odi.14138.
43. Zhang, C.; Wang, Y.; Liao, W.; Liang, T.; Liu, W.; Xie, J.; Wang, X.; Yang, P.; Lu, W.; Zhang, X. MUC1 Deficiency Induces the Nasal Epithelial Barrier Dysfunction via RBFOX3 Shortage Augments Ubiquitin-Proteasomal Degradation in Allergic Rhinitis Pathogenesis. *Allergy* **2022**, doi:10.1111/all.15235.
44. Xu, C.P.; Palazzolo, D.L.; Cuadra, G.A. Mechanistic Effects of E-Liquids on Biofilm Formation and Growth of Oral Commensal Streptococcal Communities: Effect of Flavoring Agents. *Dent J (Basel)* **2022**, *10*, 85, doi:10.3390/dj10050085.
45. Fischman, J.S.; Sista, S.; Lee, D.; Cuadra, G.A.; Palazzolo, D.L. Flavorless vs. Flavored Electronic Cigarette-Generated Aerosol and E-Liquid on the Growth of Common Oral Commensal Streptococci. *Front Physiol* **2020**, *11*, 585416, doi:10.3389/fphys.2020.585416.
46. Palazzolo, D.L.; Nelson, J.M.; Ely, E.A.; Crow, A.P.; Distin, J.; Kunigelis, S.C. The Effects of Electronic Cigarette (ECIG)-Generated Aerosol and Conventional Cigarette Smoke on the Mucociliary Transport Velocity (MTV) Using the Bullfrog (R. Catesbiana) Palate Paradigm. *Front Physiol* **2017**, *8*, 1023, doi:10.3389/fphys.2017.01023.
47. Ramenzoni, L.L.; Schneider, A.; Fox, S.C.; Meyer, M.; Meboldt, M.; Attin, T.; Schmidlin, P.R. Cytotoxic and Inflammatory Effects of Electronic and Traditional Cigarettes on Oral Gingival Cells Using a Novel Automated Smoking Instrument: An In Vitro Study. *Toxics* **2022**, *10*, 179, doi:10.3390/toxics10040179.
48. Cátala-Valentín, A.R.; Almeda, J.; Bernard, J.N.; Cole, A.M.; Cole, A.L.; Moore, S.D.; Andl, C.D. E-Cigarette Aerosols Promote Oral S. Aureus Colonization by Delaying an Immune Response and Bacterial Clearing. *Cells* **2022**, *11*, 773, doi:10.3390/cells11050773.
49. Pagano, S.; Negri, P.; Coniglio, M.; Bruscoli, S.; Di Michele, A.; Marchetti, M.C.; Valenti, C.; Gambelunghe, A.; Fanasca, L.; Billi, M.; et al. Heat-Not-Burn Tobacco (IQOS), Oral Fibroblasts and Keratinocytes: Cytotoxicity, Morphological Analysis, Apoptosis and Cellular Cycle. An in Vitro Study. *J Periodontal Res* **2021**, *56*, 917–928, doi:10.1111/jre.12888.
50. Tellez, C.S.; Juri, D.E.; Phillips, L.M.; Do, K.; Yingling, C.M.; Thomas, C.L.; Dye, W.W.; Wu, G.; Kishida, S.; Kiyono, T.; et al. Cytotoxicity and Genotoxicity of E-Cigarette Generated Aerosols Containing Diverse Flavoring Products and Nicotine in Oral Epithelial Cell Lines. *Toxicol Sci* **2021**, *179*, 220–228, doi:10.1093/toxsci/kfaa174.
51. Beklen, A.; Uckan, D. Electronic Cigarette Liquid Substances Propylene Glycol and Vegetable Glycerin Induce an Inflammatory Response in Gingival Epithelial Cells. *Hum Exp Toxicol* **2021**, *40*, 25–34, doi:10.1177/0960327120943934.
52. Stratified Epithelium Available online: https://www.kenhub.com/en/library/anatomy/stratified-epithelium (accessed on 16 June 2022).
53. Moffatt-Jauregui, C.E.; Robinson, B.; de Moya, A.V.; Brockman, R.D.; Roman, A.V.; Cash, M.N.; Culp, D.J.; Lamont, R.J. Establishment and Characterization of a Telomerase Immortalized Human Gingival Epithelial Cell Line. *J Periodontal Res* **2013**, *48*, 10.1111/jre.12059, doi:10.1111/jre.12059.
54. Oda, D.; Watson, E. Human Oral Epithelial Cell Culture I. Improved Conditions for Reproducible Culture in Serum-Free Medium. *In Vitro Cell Dev Biol* **1990**, *26*, 589–595, doi:10.1007/BF02624208.
55. Morino, T.; Takagi, R.; Yamamoto, K.; Kojima, H.; Yamato, M. Explant Culture of Oral Mucosal Epithelial Cells for Fabricating Transplantable Epithelial Cell Sheet. *Regen Ther* **2018**, *10*, 36–45, doi:10.1016/j.reth.2018.10.006.
56. Groeger, S.; Meyle, J. Oral Mucosal Epithelial Cells. *Frontiers in Immunology* **2019**, *10*.
57. Kasai, Y.; Sugiyama, H.; Takagi, R.; Kondo, M.; Owaki, T.; Namiki, H.; Okano, T.; Takeda, N.; Yamato, M. Brush Biopsy of Human Oral Mucosal Epithelial Cells as a Quality Control of the Cell Source for Fabrication of Transplantable Epithelial Cell Sheets for Regenerative Medicine. *Regenerative Therapy* **2016**, *4*, 71–77, doi:10.1016/j.reth.2016.02.008.
58. Pelaez-Prestel, H.F.; Sanchez-Trincado, J.L.; Lafuente, E.M.; Reche, P.A. Immune Tolerance in the Oral Mucosa. *Int J Mol Sci* **2021**, *22*, 12149, doi:10.3390/ijms222212149.
59. Forslind, B. Quantitative X-Ray Microanalysis of Skin. Particle Probe Evaluation of the Skin Barrier Function. *Acta Derm Venereol Suppl (Stockh)* **1987**, *134*, 1–8.
60. Forslind, B.; Lindberg, M.; Malmqvist, K.G.; Pallon, J.; Roomans, G.M.; Werner-Linde, Y. Human Skin Physiology Studied by Particle Probe Microanalysis. *Scanning Microsc* **1995**, *9*, 1011–1025; discussion 1025-1026.
61. Forslind, B.; Lindberg, M.; Roomans, G.M.; Pallon, J.; Werner-Linde, Y. Aspects on the Physiology of Human Skin: Studies Using Particle Probe Analysis. *Microsc Res Tech* **1997**, *38*, 373–386, doi:10.1002/(SICI)1097-0029(19970815)38:4<373::AID-JEMT5>3.0.CO;2-K.

62. Pallon, J.; Malmqvist, K.G.; Werner-Linde, Y.; Forslind, B. Pixe Analysis of Pathological Skin with Special Reference to Psoriasis and Atopic Dry Skin. *Cell Mol Biol (Noisy-le-grand)* **1996**, *42*, 111–118.
63. Leinonen, P.T.; Hägg, P.M.; Peltonen, S.; Jouhilahti, E.-M.; Melkko, J.; Korkiamäki, T.; Oikarinen, A.; Peltonen, J. Reevaluation of the Normal Epidermal Calcium Gradient, and Analysis of Calcium Levels and ATP Receptors in Hailey–Hailey and Darier Epidermis. *J Invest Dermatol* **2009**, *129*, 1379–1387, doi:10.1038/jid.2008.381.
64. Leonardo, T.R.; Shi, J.; Chen, D.; Trivedi, H.M.; Chen, L. Differential Expression and Function of Bicellular Tight Junctions in Skin and Oral Wound Healing. *Int J Mol Sci* **2020**, *21*, E2966, doi:10.3390/ijms21082966.
65. Ye, P.; Harty, D.; Commandeur, Z.; Hunter, N. Binding of Streptococcus Gordonii to Oral Epithelial Monolayers Increases Paracellular Barrier Function. *Microb Pathog* **2013**, *56*, 53–59, doi:10.1016/j.micpath.2012.11.004.
66. Chen, W.; Alshaikh, A.; Kim, S.; Kim, J.; Chun, C.; Mehrazarin, S.; Lee, J.; Lux, R.; Kim, R.H.; Shin, K.H.; et al. Porphyromonas Gingivalis Impairs Oral Epithelial Barrier through Targeting GRHL2. *J Dent Res* **2019**, *98*, 1150–1158, doi:10.1177/0022034519865184.
67. Lagha, A.B.; Groeger, S.; Meyle, J.; Grenier, D. Green Tea Polyphenols Enhance Gingival Keratinocyte Integrity and Protect against Invasion by Porphyromonas Gingivalis. *Pathog Dis* **2018**, *76*, doi:10.1093/femspd/fty030.
68. Guo, W.; Wang, P.; Liu, Z.-H.; Ye, P. Analysis of Differential Expression of Tight Junction Proteins in Cultured Oral Epithelial Cells Altered by Porphyromonas Gingivalis, Porphyromonas Gingivalis Lipopolysaccharide, and Extracellular Adenosine Triphosphate. *Int J Oral Sci* **2018**, *10*, e8, doi:10.1038/ijos.2017.51.
69. Rosace, D.; Gomez-Casado, C.; Fernandez, P.; Perez-Gordo, M.; Dominguez, M.D.C.; Vega, A.; Belver, M.T.; Ramos, T.; Vega, F.; Marco, G.; et al. Profilin-Mediated Food-Induced Allergic Reactions Are Associated with Oral Epithelial Remodeling. *J Allergy Clin Immunol* **2019**, *143*, 681-690.e1, doi:10.1016/j.jaci.2018.03.013.
70. Najarro, K.M.; Boe, D.M.; Walrath, T.M.; Mullen, J.E.; Paul, M.T.; Frankel, J.H.; Hulsebus, H.J.; Idrovo, J.-P.; McMahan, R.H.; Kovacs, E.J. Advanced Age Exacerbates Intestinal Epithelial Permeability after Burn Injury in Mice. *Experimental Gerontology* **2022**, *158*, 111654, doi:10.1016/j.exger.2021.111654.
71. Gendler, S.J. MUC1, the Renaissance Molecule. *J Mammary Gland Biol Neoplasia* **2001**, *6*, 339–353, doi:10.1023/a:1011379725811.
72. Wreschner, D.H.; McGuckin, M.A.; Williams, S.J.; Baruch, A.; Yoeli, M.; Ziv, R.; Okun, L.; Zaretsky, J.; Smorodinsky, N.; Keydar, I.; et al. Generation of Ligand-Receptor Alliances by "SEA" Module-Mediated Cleavage of Membrane-Associated Mucin Proteins. *Protein Sci* **2002**, *11*, 698–706, doi:10.1110/ps.16502.
73. Levitin, F.; Stern, O.; Weiss, M.; Gil-Henn, C.; Ziv, R.; Prokocimer, Z.; Smorodinsky, N.I.; Rubinstein, D.B.; Wreschner, D.H. The MUC1 SEA Module Is a Self-Cleaving Domain. *J Biol Chem* **2005**, *280*, 33374–33386, doi:10.1074/jbc.M506047200.
74. Parry, S.; Silverman, H.S.; McDermott, K.; Willis, A.; Hollingsworth, M.A.; Harris, A. Identification of MUC1 Proteolytic Cleavage Sites in Vivo. *Biochem Biophys Res Commun* **2001**, *283*, 715–720, doi:10.1006/bbrc.2001.4775.
75. Arcasoy, S.M.; Latoche, J.; Gondor, M.; Watkins, S.C.; Henderson, R.A.; Hughey, R.; Finn, O.J.; Pilewski, J.M. MUC1 and Other Sialoglycoconjugates Inhibit Adenovirus-Mediated Gene Transfer to Epithelial Cells. *Am J Respir Cell Mol Biol* **1997**, *17*, 422–435, doi:10.1165/ajrcmb.17.4.2714.
76. Walters, R.W.; Pilewski, J.M.; Chiorini, J.A.; Zabner, J. Secreted and Transmembrane Mucins Inhibit Gene Transfer with AAV4 More Efficiently than AAV5. *J Biol Chem* **2002**, *277*, 23709–23713, doi:10.1074/jbc.M200292200.
77. Lillehoj, E.P.; Hyun, S.W.; Kim, B.T.; Zhang, X.G.; Lee, D.I.; Rowland, S.; Kim, K.C. Muc1 Mucins on the Cell Surface Are Adhesion Sites for Pseudomonas Aeruginosa. *Am J Physiol Lung Cell Mol Physiol* **2001**, *280*, L181-187, doi:10.1152/ajplung.2001.280.1.L181.
78. Lindén, S.K.; Sheng, Y.H.; Every, A.L.; Miles, K.M.; Skoog, E.C.; Florin, T.H.J.; Sutton, P.; McGuckin, M.A. MUC1 Limits Helicobacter Pylori Infection Both by Steric Hindrance and by Acting as a Releasable Decoy. *PLoS Pathog* **2009**, *5*, e1000617, doi:10.1371/journal.ppat.1000617.
79. Lima, B.P.; Davies, J.R.; Wickström, C.; Johnstone, K.F.; Hall, J.W.; Svensater, G.; Herzberg, M.C. Streptococcus Gordonii Poised for Glycan Feeding through a MUC5B-Discriminating, Lipoteichoic Acid-Mediated Outside-In Signaling Circuit. *J Bacteriol* **2022**, *204*, e0011822, doi:10.1128/jb.00118-22.
80. Culp, D.J.; Robinson, B.; Cash, M.N.; Bhattacharyya, I.; Stewart, C.; Cuadra-Saenz, G. Salivary Mucin 19 Glycoproteins: Innate Immune Functions in Streptococcus Mutans-Induced Caries in Mice and Evidence for Expression in Human Saliva. *J Biol Chem* **2015**, *290*, 2993–3008, doi:10.1074/jbc.M114.597906.
81. Frenkel, E.S.; Ribbeck, K. Salivary Mucins Protect Surfaces from Colonization by Cariogenic Bacteria. *Appl Environ Microbiol* **2015**, *81*, 332–338, doi:10.1128/AEM.02573-14.
82. Ling, L.-Q.R.; Lin, Z.; Paolini, R.; Farah, C.S.; McCullough, M.; Lim, M.A.W.T.; Celentano, A. Commonly Prescribed Anticoagulants Exert Anticancer Effects in Oral Squamous Cell Carcinoma Cells In Vitro. *Biology (Basel)* **2022**, *11*, 596, doi:10.3390/biology11040596.
83. Dennis, M.; Wang, G.; Luo, J.; Lin, Y.; Dohadwala, M.; Sidell, D.; DeConde, A.; Abemayor, E.; Elashoff, D.A.; Sharma, S.; et al. Snail Controls the Mesenchymal Phenotype and Drives Erlotinib Resistance in Oral Epithelial and HNSCC Cells. *Otolaryngol Head Neck Surg* **2012**, *147*, 726–732, doi:10.1177/0194599812446407.
84. Shaikh, Z.N.; Alqahtani, A.; Almela, T.; Franklin, K.; Tayebi, L.; Moharamzadeh, K. Effects of Electronic Cigarette Liquid on Monolayer and 3D Tissue-Engineered Models of Human Gingival Mucosa. *J Adv Periodontol Implant Dent* **2019**, *11*, 54–62, doi:10.15171/japid.2019.010.

85. Alanazi, H.; Semlali, A.; Chmielewski, W.; Rouabhia, M. E-Cigarettes Increase Candida Albicans Growth and Modulate Its Interaction with Gingival Epithelial Cells. *International Journal of Environmental Research and Public Health* **2019**, *16*, 294, doi:10.3390/ijerph16020294.
86. Catala-Valentin, A.; Bernard, J.N.; Caldwell, M.; Maxson, J.; Moore, S.D.; Andl, C.D. E-Cigarette Aerosol Exposure Favors the Growth and Colonization of Oral Streptococcus Mutans Compared to Commensal Streptococci. *Microbiol Spectr 10*, e02421-21, doi:10.1128/spectrum.02421-21.
87. Cátala-Valentín, A.R.; Almeda, J.; Bernard, J.N.; Cole, A.M.; Cole, A.L.; Moore, S.D.; Andl, C.D. E-Cigarette Aerosols Promote Oral S. Aureus Colonization by Delaying an Immune Response and Bacterial Clearing. *Cells* **2022**, *11*, 773, doi:10.3390/cells11050773.
88. Yessentayeva, S.Y.; Orakbay, L.Z.; Adilhanova, A.; Yessimov, N. Approaches to the Use of Stem Cells in Regenerative Medicine. *Anal Biochem* **2022**, *645*, 114608, doi:10.1016/j.ab.2022.114608.
89. Moysidou, C.-M.; Barberio, C.; Owens, R.M. Advances in Engineering Human Tissue Models. *Front Bioeng Biotechnol* **2020**, *8*, 620962, doi:10.3389/fbioe.2020.620962.
90. Klausner, M.; Handa, Y.; Aizawa, S. In Vitro Three-Dimensional Organotypic Culture Models of the Oral Mucosa. *In Vitro Cell Dev Biol Anim* **2021**, *57*, 148–159, doi:10.1007/s11626-020-00539-1.
91. Gibbs, S.; Roffel, S.; Meyer, M.; Gasser, A. Biology of Soft Tissue Repair: Gingival Epithelium in Wound Healing and Attachment to the Tooth and Abutment Surface. *Eur Cell Mater* **2019**, *38*, 63–78, doi:10.22203/eCM.v038a06.
92. Xu, H.; Zhong, L.; Deng, J.; Peng, J.; Dan, H.; Zeng, X.; Li, T.; Chen, Q. High Expression of ACE2 Receptor of 2019-NCoV on the Epithelial Cells of Oral Mucosa. *Int J Oral Sci* **2020**, *12*, 1–5, doi:10.1038/s41368-020-0074-x.
93. Daniell, H.; Nair, S.K.; Esmaeili, N.; Wakade, G.; Shahid, N.; Ganesan, P.K.; Islam, M.R.; Shepley-McTaggart, A.; Feng, S.; Gary, E.N.; et al. Debulking SARS-CoV-2 in Saliva Using Angiotensin Converting Enzyme 2 in Chewing Gum to Decrease Oral Virus Transmission and Infection. *Molecular Therapy* **2021**, *0*, doi:10.1016/j.ymthe.2021.11.008.
94. Moller, H.J.; Poulsen, J.H. Improved Method for Silver Staining of Glycoproteins in Thin Sodium Dodecyl Sulfate Polyacrylamide Gels. *Analytical Biochemistry* **1995**, *226*, 371–374, doi:10.1006/abio.1995.1238.
95. Suarez-Arnedo, A.; Torres Figueroa, F.; Clavijo, C.; Arbeláez, P.; Cruz, J.C.; Muñoz-Camargo, C. An Image J Plugin for the High Throughput Image Analysis of in Vitro Scratch Wound Healing Assays. *PLoS One* **2020**, *15*, e0232565, doi:10.1371/journal.pone.0232565.
96. Schindelin, J.; Rueden, C.T.; Hiner, M.C.; Eliceiri, K.W. The ImageJ Ecosystem: An Open Platform for Biomedical Image Analysis. *Mol Reprod Dev* **2015**, *82*, 518–529, doi:10.1002/mrd.22489.